Smart Structures and Systems, *Vol. 22, No. 1 (2018) 105-120*
DOI: https://doi.org/10.12989/sss.2018.22.1.105

Non-linear free and forced vibration analysis of sandwich nano-beam with FG-CNTRC face-sheets based on nonlocal strain gradient theory

Ali Ghorbanpour Arani*, Mahmoud Pourjamshidian[a] and Mohammad Arefi[b]

Department of Solid Mechanics, Faculty of Mechanical Engineering, University of Kashan, Postal Code: 87317-53153, Kashan, Iran

(Received December 29, 2016, Revised December 15, 2017, Accepted April 16, 2018)

Abstract. In this paper, the nonlinear free and forced vibration responses of sandwich nano-beams with three various functionally graded (FG) patterns of reinforced carbon nanotubes (CNTs) face-sheets are investigated. The sandwich nano-beam is resting on nonlinear Visco-elastic foundation and is subjected to thermal and electrical loads. The nonlinear governing equations of motion are derived for an Euler-Bernoulli beam based on Hamilton principle and von Karman nonlinear relation. To analyze nonlinear vibration, Galerkin's decomposition technique is employed to convert the governing partial differential equation (PDE) to a nonlinear ordinary differential equation (ODE). Furthermore, the Multiple Times Scale (MTS) method is employed to find approximate solution for the nonlinear time, frequency and forced responses of the sandwich nano-beam. Comparison between results of this paper and previous published paper shows that our numerical results are in good agreement with literature. In addition, the nonlinear frequency, force response and nonlinear damping time response is carefully studied. The influences of important parameters such as nonlocal parameter, volume fraction of the CNTs, different patterns of CNTs, length scale parameter, Visco-Pasternak foundation parameter, applied voltage, longitudinal magnetic field and temperature change are investigated on the various responses. One can conclude that frequency of FG-AV pattern is greater than other used patterns.

Keywords: euler-bernoulli beam theory; reinforcement carbon nano-tube composite; sandwich beams; nonlocal strain gradient theory; non-linear vibration

1. Introduction

In recent years, remarkable development in engineering materials has caused to create new materials such as the carbon nanotube reinforcement composites (CNTRCs). Carbon nanotubes can be used to reinforce the polymer composites (Esawi and Farag 2007). Combination of nano tubes and CNTs leads to excellent properties for various applications. An investigation on the related references indicates that properties of the some materials can improve using compounding with CNTs (Amal and Mahmoud 2007). It is noted that these improved properties is depending on the base materials, type of the CNTs and their distribution patterns. Developing of these material properties makes that the CNTRCs achieve a wide applications in micro and nano systems (Ashrafi and Hubert 2006). Recently, many researchers focused on the problems that concern with FG-CNTRC. For example thermal stresses analysis, linear and nonlinear vibration, the dynamic response in thermal environments, the nonlinear bending response subjected to transverse loads under thermal environments and other problems in this case were studied by some researchers (Ghorbanpour Arani *et al.* 2012, Ansari *et al.* 2014, Ghorbanpour Arani *et al.* 2015, Mohammadimehr and Mostafavifar 2016, Mohammadimehr *et al.* 2016, Wu et al. 2016). The thermo mechanical properties of nano-composites investigated by Fidelus *et al.* (2005) in detail. They assumed nano-composite made from combination of epoxy and SWCNTs and multi-walled (MW) CNTs oriented randomly. In the other research the static behavior of FG-CNTRC plate was studied by Alibeigloo (2014). Li *et al.* (2016) in their investigation developed molecular models included Fe atoms. The abrasion rate and friction coefficient are examined with sliding the polymer matrix and nano-rod on each other in the presence of normal loadings. Formica *et al.* (2010) analyzed the vibration characteristics of CNTRC. They used the Eshelby–Mori–Tanaka approach in order to simulate continuum model. In according to their research, the natural frequencies of the rubber reinforced by CNTs enhances up to 500 percent. The response of the FG-CNTRC beam due to impacting mass was represented by Jam *et al.* (2015). They employed the Timoshenko beam theory to indicate the kinematics relations of the beam. Shen and Zhang (2010) studied post buckling and thermal buckling of the plate reinforced by SWCNTs and exposed to temperature change. They concluded that there is no initial thermal post buckling strength in plate made of CNTRC with intermediate nanotube volume fraction. Wattanasakulpong *et al.* (2013) studied the vibration,

*Corresponding author, Professor
E-mail: aghorban@kashanu.ac.ir
[a] Ph.D. Student
E-mail: jamshidian1989@gmail.com
[b] Assistant Professor
E-mail: arefi@kashanu.ac.ir

Copyright © 2018 Techno-Press, Ltd.

ISSN: 1738-1584 (Print), 1738-1991 (Online)

bending and buckling in beam made of CNTRC. In their work the effects of some parameters such as spring constant factors, several aspects of beam and carbon nanotube volume fraction were discussed. The vibration of beam made of CNTRC with temperature variation and surface-bonded piezoelectric layers was studied by Rafiee *et al.* (2013). Through a comprehensive parametric study, they investigated the influences of the main parameters on the linear and nonlinear frequencies. The free vibration and bending of the CNTRC sandwich plate based on higher-order theory were studied by Natarajan *et al.* (2014). Rafiee *et al.* (2014) carried out an investigation on nonlinear stability and resonance response of the imperfect plate made of piezoelectric FG-CNTRC subjected to various combined electrical and thermal loads. Another research in case of nano-composite reinforced by SWCNTs was accomplished by Ke *et al.* (2010) on nonlinear free vibration of the Timoshenko beam with considering von Kármán geometric nonlinearity. Also according to study that implemented by Mohammadimehr *et al*. (2015), the influences of the various pattern of the of SWCNTs as: UD, FG-V, FG-X and FG-O on dimensionless natural frequency were studied on the free vibration of visco-elastic double-bonded polymeric nano-composite plate. Researchers have found that application of micro/nano-composites in micro/nano electromechanical systems leads to important and novel responses to raised problem in this context.

Recently, the influences of the small materials length scales parameters were considered by the researchers in their investigations in case of the nano and micro structures. To have a precision analysis in small structures, it is necessary to consider small scales parameters in the governing equation of motion of the structures in order to model the mechanical or physical properties (Li *et al.* 2015). For example, the continuum mechanics theory that used in research concerning with nano/micro systems include classical continuum models (Shakeri *et al.* 2006, Zhang and Paulino 2007), nonlocal continuum theory (Simsek and Yurtcu 2013, Reddy *et al*. 2014, Nazemnezhad *et al.* 2014, Ebrahimi and Salari 2015, Kiani 2015, Niknam and Aghdam 2015, Pang *et al*. 2015, Rahmani and Jandaghian 2015, Salehipour *et al.* 2015), strain gradient theory (Akgoz and Civalek 2013, Tajalli *et al.* 2013, Gholami *et al.* 2014, Setoodeh and Afrahim 2014), and modified couple stress models (Nateghi and Salamat-talab 2013, Akgoz and Civalek 2014, Ansari *et al.* 2014, Jung and Han 2015). Based on the nonlocal strain gradient theory, Liew et al. (2008) analyzed the wave propagation in a SWCNT and obtained results comparing with results achieved by molecular dynamics simulations. Some magneto-electro-thermo-elastic analysis of nano-beams can be observed in literature (Arefi *et al.* 2018, Arefi and Zenkour 2016, Arefi and Zenkour 2017a, Zenkour and Arefi 2017). The effect of surface elasticity was accounted in the nonlocal formulation of nanobeams (Arefi *et al.* 2018, Arefi 2016, Arefi and Zenkour 2017c). Vibration and bending analysis of sandwich structures in terms of applied voltage based on various lower- and higher-order shear deformation theories were studied by Arefi and Zenkour (2017a, b, d, e).

Comprehensive investigation on literature mentioned above indicates that there is no published work about free damping and nonlinear free and forced vibration of the sandwich nano-beam with face-sheets made of FG-CNTRC resting on Visco-Pasternak elastic foundation in electro-thermal environment. The present analysis is performed based on nonlocal strain gradient theory, von Karman nonlinearity and Hamilton's principle. The influence of some significant parameters such as small scales parameter, electrical and thermal loads and various patterns of FG-CNTRC are discussed on the nonlinear free and forced vibration characteristics of the sandwich nano-beam in detail.

2. Sandwich nano-beams with face-sheets made of the FG-CNTRC

The structure of sandwich nano-beam with face-sheets made of the FG-CNTRC is represented in Fig. 1. Regarding to this figure, it is assumed that core of the beam and matrix of the face-sheets are made of viscoelastic piezoelectric materials. CNTs aligned along thickness direction according to three patterns namely $FG(AV)$, $FG(VA)$and UD.

In different published study, properties of CNTRCs calculated using the Mori–Tanaka scheme or with employing others rule of mixtures that in present investigation the simple rule of mixtures with correction factors is applied (Natarajan *et al*. 2014, Ghorbanpour Arani *et al.* 2016). According to the rule of mixture, the properties of the materials made of the CNTRC (Young's modulus (E^{rc}), expansion coefficient (α^{rc}), visco-elastic coefficient (τ_d^{rc}) and density (ρ^{rc}) of the reinforced composite) are expressed by (Rafiee *et al.* 2014)

$$\begin{aligned} E^{rc} &= \eta_1 V_{cn} E_{11}^{CN} + V_m E^m \\ \alpha^{rc} &= V_{cn} \alpha_{11}^{CN} + V_m \alpha^m \\ \tau_d^{rc} &= V_{cn} \tau_d^{CN} + V_m \tau_d^m \\ \rho^{rc} &= V_{cn} \rho^{CN} + V_m \rho^m \end{aligned} \tag{1}$$

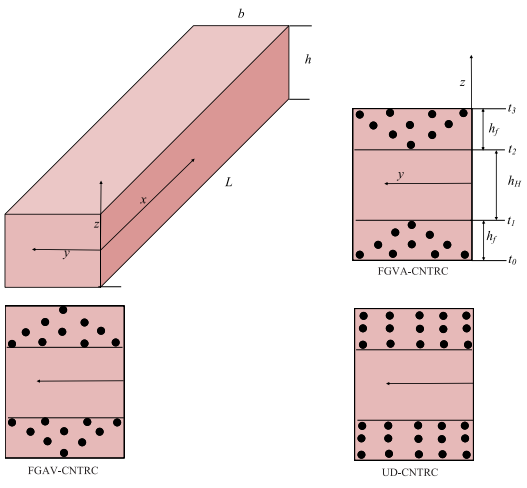

Fig. 1 Sandwich nano-beam with CNTRC face-sheets

In which, η_1, E_{11}^{CN}, α_{11}^{CN}, τ_d^{CN} and ρ_{11}^{CN} are the CNT efficiency parameter, the Young's modulus, the expansion coefficient, the visco-elastic coefficient and density of the CNTs, respectively and E^m, α^m, τ_d^m and ρ^m are the matrix properties. Furthermore, V_{CN} and V_m are volume fractions of the CNTs and matrix that related by $V_{CN} + V_m = 1$ (Shen and Zhang 2012). The CNTs distributed and aligned along the thickness direction of the top and bottom face-sheets according to following formulations

$$\begin{aligned} &V_{CN}^t = 2\frac{(t_2-\bar{z})}{(t_2-t_3)}V_{CN}^* \\ &V_{CN}^b = 2\frac{(t_1+\bar{z})}{(t_1-t_0)}V_{CN}^*, \quad \Rightarrow \quad \textit{for FG(VA) pattern} \\ &V_{CN}^t = 2V_{CN}^* \\ &V_{CN}^b = 2V_{CN}^*, \quad \Rightarrow \quad \textit{for UD pattern} \\ &V_{CN}^t = 2\frac{(t_3-\bar{z})}{(t_3-t_2)}V_{CN}^* \\ &V_{CN}^b = 2\frac{(t_0+\bar{z})}{(t_0-t_1)}V_{CN}^*, \quad \Rightarrow \quad \textit{for FG(AV) pattern} \end{aligned} \tag{2}$$

Where V_{CN}^t and V_{CN}^b represent the volume fractions of the CNTs in top and bottom face-sheets, respectively and also V_{CN}^* can be calculated as

$$V_{CN}^* = \frac{w_{CN}}{w_{CN} + \left(\frac{\rho^{CN}}{\rho^m}\right) - \left(\frac{\rho^{CN}}{\rho^m}\right)w_{CN}} \tag{3}$$

In above equation, w_{CN} characterize the mass fraction of the CNTs.

3. Formulation

3.1 Equation of motion

The displacement field for Euler-Bernoulli beam is defined as

$$\begin{aligned} &\bar{u}(\bar{x},\bar{z},\bar{t}) = u_0(\bar{x},\bar{t}) - \bar{z}\frac{\partial w_0(\bar{x},\bar{t})}{\partial \bar{x}} \\ &\bar{w}(\bar{x},\bar{z},\bar{t}) = w_0(\bar{x},\bar{t}) \end{aligned} \tag{4}$$

In which, $\bar{u}$ and $\bar{w}$ are axial and transverse displacement components, u_0 and w_0 are axial and transverse displacements of mid-surface. The strain-displacement relation based on nonlinear Von-Karman relation considering the thermal strain is expressed as

$$\varepsilon_{\bar{x}\bar{x}} = \frac{\partial u_0}{\partial \bar{x}} - \bar{z}\frac{\partial^2 w_0}{\partial \bar{x}^2} + \frac{1}{2}\left(\frac{\partial w_0}{\partial \bar{x}}\right)^2 - \alpha(\bar{z})\Delta T \tag{5}$$

In which, ΔT is the increment of temperature (T_0) that is equal to $\Delta T = T - T_0$. Regarding to the Kelvin–Voigt viscoelastic damping model, the strain-stress relation for reinforcement composite face-sheets is defined as (Li *et al.* 2015)

$$\sigma_{\bar{x}\bar{x}}^{rc} = E^{rc}(\bar{z})\left(1-\tau_d^{rc}(\bar{z})\frac{\partial}{\partial \bar{t}}\right)\left(\begin{array}{l}\frac{\partial u_0}{\partial \bar{x}} - z\frac{\partial^2 w_0}{\partial \bar{x}^2} + \\ \frac{1}{2}\left(\frac{\partial w_0}{\partial \bar{x}}\right)^2 - \alpha(\bar{z})\Delta T\end{array}\right) \tag{6}$$

Considering the applied voltage on piezoelectric core layer, the strain-stress relation of the core is specified as

$$\sigma_{\bar{x}\bar{x}}^{p} = E^m\left(1+\tau_d^m\frac{\partial}{\partial \bar{t}}\right)\left(\begin{array}{l}\frac{\partial u_0}{\partial \bar{x}} - \bar{z}\frac{\partial^2 w_0}{\partial \bar{x}^2} + \\ \frac{1}{2}\left(\frac{\partial w_0}{\partial \bar{x}}\right)^2 - \alpha(\bar{z})\Delta T - d_{31}E_{\bar{z}}\end{array}\right) \tag{7}$$

In which $d_{31}$is the piezoelectric strain constant (Liew *et al.* 2003). Because of the small value of thickness of the piezoelectric core, the relation between electric field and applied voltage is expressed as (Liew *et al.* 2003, Rafiee *et al.* 2013)

$$E_{\bar{z}} = \frac{V(\bar{t})}{h_c} \tag{8}$$

The procedure extracted above phrase is represented in Appendix A1 in detail. In Eq. (8) h_c and $V(\bar{t})$ are thickness of the piezoelectric core and applied voltage in $\bar{z}$ direction of the core, respectively. In general, the properties associated with the core and face-sheets represent with c and rc superscripts, respectively. In order to derive the governing equation of motion, the Hamilton's principle is employed as follow

$$0 = \int_0^T (\delta T - \delta U + \delta W)d\bar{t} \tag{9}$$

Where δU, δT and δW are the density of the strain energy, the kinetic energy, and the work done by external forces, respectively. The virtual strain energy δU is calculated as

$$\delta U = \int_0^L \int_A \sigma_{\bar{x}\bar{x}}\delta\varepsilon_{\bar{x}\bar{x}}dAd\bar{x} \tag{10}$$

Virtual kinetic energy is represented as

$$\delta T = \int_0^L \int_A \rho(\bar{z})\left(\frac{\partial \bar{u}}{\partial \bar{t}}\frac{\partial \bar{u}}{\partial \bar{t}} + \frac{\partial \bar{w}}{\partial \bar{t}}\frac{\partial \bar{w}}{\partial \bar{t}}\right)dAd\bar{x} \tag{11}$$

The virtual work done by the external forces is written as

$$\delta W = \int_0^L \left(F\delta u_0 + Q\delta w_0 + \bar{N}_0\frac{\partial w_0}{\partial \bar{x}}\frac{\partial \delta w_0}{\partial \bar{x}}\right)d\bar{x} \tag{12}$$

Where F and Q are the axial force and transverse force per unit length respectively, and $\bar{N}_0$ is the axial compressive or pretension force. Substitution of Eqs. (4) and (5) into Eqs. (10)-(12) and consequently into Eq. (9), yields the governing equations of motions as

$$\delta u_0 : \frac{\partial N_{\bar{x}}}{\partial \bar{x}} + F = m_0 \frac{\partial^2 u_0}{\partial \bar{t}^2}$$
$$\delta w_0 : \frac{\partial^2 M_{\bar{x}}}{\partial \bar{x}^2} + \frac{\partial}{\partial \bar{x}}\left(N_{\bar{x}} \frac{\partial w_0}{\partial \bar{x}} \right) - \frac{\partial}{\partial \bar{x}}\left(\bar{N}_0 \frac{\partial w_0}{\partial \bar{x}} \right) + Q = \quad (13)$$
$$m_0 \frac{\partial^2 w_0}{\partial \bar{t}^2} - m_2 \frac{\partial^4 w_0}{\partial \bar{t}^2 \partial \bar{x}^2}$$

Where, $N_{\bar{x}}$ and $M_{\bar{x}}$ symbolize force and moment resultants, respectively. Due to changing the density along the z direction, two parameters m0 and m_2 are calculated as

$$m_0 = \int_{-h/2}^{h/2} \rho(\bar{z})\, d\bar{z} = \left(\int_{t_0}^{t_1} \rho^{rc}(\bar{z})\, d\bar{z} + \int_{t_1}^{t_2} \rho^{c}(\bar{z})\, d\bar{z} + \int_{t_2}^{t_3} \rho^{rc}(\bar{z})\, d\bar{z} \right)$$
$$m_2 = \int_{-h/2}^{h/2} z^2 \rho(\bar{z})\, d\bar{z} = \left(\int_{t_0}^{t_1} \bar{z}^2 \rho^{rc}(\bar{z})\, d\bar{z} + \int_{t_1}^{t_2} \bar{z}^2 \rho^{c}(\bar{z})\, dz + \int_{t_2}^{t_3} \bar{z}^2 \rho^{rc}(\bar{z})\, d\bar{z} \right) \quad (14)$$

And $N_{\bar{x}}$ and $M_{\bar{x}}$ are expressed as

$$N_{\bar{x}} = \int_{-h/2}^{h/2} \sigma_{\bar{x}\bar{x}}(\bar{z})\, d\bar{z} = \left(\int_{t_0}^{t_1} \sigma_{\bar{x}\bar{x}}^{rc} d\bar{z} + \int_{t_1}^{t_2} \sigma_{\bar{x}\bar{x}}^{c} d\bar{z} + \int_{t_2}^{t_3} \sigma_{\bar{x}\bar{x}}^{rc} d\bar{z} \right)$$
$$M_{\bar{x}} = \int_{-h/2}^{h/2} \bar{z}\sigma_{\bar{x}\bar{x}}(\bar{z})\, d\bar{z} = \left(\int_{t_0}^{t_1} \bar{z}\sigma_{\bar{x}\bar{x}}^{rc} d\bar{z} + \int_{t_1}^{t_2} \bar{z}\sigma_{\bar{x}\bar{x}}^{c} d\bar{z} + \int_{t_2}^{t_3} \bar{z}\sigma_{\bar{x}\bar{x}}^{rc} d\bar{z} \right) \quad (15)$$

In according to nonlocal strain gradient theory (Li and Hu 2016), the constitutive relation between stress and strain are expressed as

$$\left(1 - (\bar{e}_0 \bar{a})^2 \nabla^2\right) t_{\bar{x}\bar{x}} = \left(1 + \tau_d \frac{\partial}{\partial \bar{t}}\right) E \left(1 - \bar{l}_m^2 \nabla^2\right) \varepsilon_{\bar{x}\bar{x}} \quad (16)$$

In above equation, t_{xx} is the stress, $\nabla^2 = \partial^2/\partial \bar{x}^2$ is the Laplacian operator, $\bar{e}_0 \bar{a}$ represents the nonlocal parameters and $\bar{l}_m$ characterize the strain gradient length scale parameter to incorporate the small scale characteristics of the micro/nano structures in the governing equation of motion. In present investigation, the explicit form of the last equation can be rewritten as follows

$$\sigma_{\bar{x}\bar{x}} - (\bar{e}_0 \bar{a})^2 \frac{\partial^2 \sigma_{\bar{x}\bar{x}}}{\partial \bar{x}^2} = \left(1 + \tau_d(\bar{z}) \frac{\partial}{\partial \bar{t}}\right) E(\bar{z}) \left[\frac{\partial u_0}{\partial \bar{x}} - \bar{z} \frac{\partial^2 w_0}{\partial \bar{x}^2} + \frac{1}{2}\left(\frac{\partial w_0}{\partial \bar{x}} \right)^2 - \alpha(\bar{z}) \Delta T - d_{31} E_{\bar{z}} \right] - \left(1 + \tau_d(\bar{z}) \frac{\partial}{\partial \bar{t}}\right) \times E(\bar{z}) \bar{l}_m^2 \left[\frac{\partial^3 u_0}{\partial \bar{x}^3} + \frac{\partial w_0}{\partial \bar{x}} \frac{\partial^3 w_0}{\partial \bar{x}^3} + \left(\frac{\partial^2 w_0}{\partial \bar{x}^2} \right)^2 - \bar{z} \frac{\partial^4 w_0}{\partial \bar{x}^4} \right] \quad (17)$$

The force and moment resultants using Eqs. (15)-(17) are expressed as the following

$$N_{\bar{x}\bar{x}} - (\bar{e}_0 \bar{a})^2 \frac{\partial^2 N_{\bar{x}\bar{x}}}{\partial \bar{x}^2} = \left(\bar{A}_{\bar{x}\bar{x}} - \bar{A}_{\bar{x}\bar{x}\tau} \frac{\partial}{\partial \bar{t}} \right) \times \left[\frac{\partial u_0}{\partial \bar{x}} - \bar{z} \frac{\partial^2 w_0}{\partial \bar{x}^2} + \frac{1}{2}\left(\frac{\partial w_0}{\partial \bar{x}} \right)^2 \right] - \bar{R}_{68} - \frac{\partial}{\partial \bar{t}} \bar{R}_{79} - \left(\bar{A}_{\bar{x}\bar{x}} - \bar{A}_{\bar{x}\bar{x}\tau} \frac{\partial}{\partial \bar{t}} \right) \bar{l}_m^2 \left[\frac{\partial^3 u_0}{\partial \bar{x}^3} + \frac{\partial w_0}{\partial \bar{x}} \frac{\partial^3 w_0}{\partial \bar{x}^3} + \left(\frac{\partial^2 w_0}{\partial \bar{x}^2} \right)^2 \right] \quad (18)$$

$$M_{\bar{x}\bar{x}} - (\bar{e}_0 \bar{a})^2 \frac{\partial^2 M_{\bar{x}\bar{x}}}{\partial \bar{x}^2} = \left(\bar{D}_{\bar{x}\bar{x}} + \bar{D}_{\bar{x}\bar{x}\tau} \frac{\partial}{\partial \bar{t}} \right) \frac{\partial^2 w_0}{\partial \bar{x}^2} - M^T - M^P - \left(\bar{D}_{\bar{x}\bar{x}} + \bar{D}_{\bar{x}\bar{x}\tau} \frac{\partial}{\partial \bar{t}} \right) \bar{l}_m^2 \frac{\partial^4 w_0}{\partial \bar{x}^4}$$

Where superscripts P and T represent thermal and electrical loads and $M^T, M^P, \bar{R}_{68}$ and $\bar{R}_{79}$ are calculated as

$$\begin{pmatrix} M^T \\ M^P \end{pmatrix} = \int_{-H/2}^{H/2} \begin{pmatrix} E(\bar{z}) \left(\left(1 + \tau_d^m \frac{\partial}{\partial \bar{t}}\right)^{\text{for middle layer}} \right. \\ \left. or \left(1 + \tau_d^{rc}(\bar{z}) \frac{\partial}{\partial \bar{t}}\right)^{\text{for FG-CNTRC facesheets}} \right) \alpha(\bar{z}) \Delta T \\ E^c \left(1 + \tau_d^m \frac{\partial}{\partial \bar{t}}\right)^{\text{for middle layer}} d_{31} E_{\bar{z}} \end{pmatrix} \bar{z}\, d\bar{z} \quad (19)$$

$$\bar{R}_{68} = \int_{-H/2}^{H/2} E(\bar{z}) \left(\alpha(\bar{z}) \Delta T + d_{31} E_{\bar{z}} \right) d\bar{z}$$
$$\bar{R}_{79} = \int_{-H/2}^{H/2} E(\bar{z}) \tau_d(\bar{z}) \left(\alpha(\bar{z}) \Delta T + d_{31} E_{\bar{z}} \right) d\bar{z}$$

It is noted that, A_{xx} and D_{xx} are the extensional and bending coefficients, respectively can be obtained as

$$\begin{Bmatrix} A_{\bar{x}\bar{x}} \\ A_{\bar{x}\bar{x}\tau} \\ D_{\bar{x}\bar{x}} \\ D_{\bar{x}\bar{x}\tau} \end{Bmatrix} = \int_{-h/2}^{h/2} \begin{Bmatrix} 1 \\ \tau(\bar{z}) \\ \bar{z}^2 \\ \bar{z}^2 \tau(\bar{z}) \end{Bmatrix} E(\bar{z})\, d\bar{z} \quad (20)$$

If the second derivatives of the $N_{\bar{x}}$ and $M_{\bar{x}}$ from Eq. (13) are substituted into Eq. (18), respectively, we will have following stress resultants

$$N_{\bar{x}\bar{x}} = \left(\bar{A}_{\bar{x}\bar{x}} + \bar{A}_{\bar{x}\bar{x}\tau} \frac{\partial}{\partial \bar{t}} \right) \left[\frac{\partial u_0}{\partial \bar{x}} - \bar{z} \frac{\partial^2 w_0}{\partial \bar{x}^2} + \frac{1}{2}\left(\frac{\partial w_0}{\partial \bar{x}} \right)^2 \right] - \bar{R}_{68} + \frac{\partial}{\partial \bar{t}} \bar{R}_{79} - \left(\bar{A}_{\bar{x}\bar{x}} + \bar{A}_{\bar{x}\bar{x}\tau} \frac{\partial}{\partial \bar{t}} \right) \bar{l}_m^2 \left[\frac{\partial^3 u_0}{\partial \bar{x}^3} + \frac{\partial w_0}{\partial \bar{x}} \frac{\partial^3 w_0}{\partial \bar{x}^3} + \left(\frac{\partial^2 w_0}{\partial \bar{x}^2} \right)^2 \right] + (\bar{e}_0 \bar{a})^2 \left\{ m_0 \frac{\partial^3 u_0}{\partial \bar{x} \partial \bar{t}^2} - \frac{\partial F}{\partial x} \right\} \quad (21)$$

$$M_{\bar{x}\bar{x}} = \left(\bar{D}_{\bar{x}\bar{x}} + \bar{D}_{\bar{x}\bar{x}\tau} \frac{\partial}{\partial \bar{t}} \right) \frac{\partial^2 w_0}{\partial \bar{x}^2} - M^T - M^P - \left(\bar{D}_{\bar{x}\bar{x}} + \bar{D}_{\bar{x}\bar{x}\tau} \frac{\partial}{\partial \bar{t}} \right) \bar{l}_m^2 \frac{\partial^4 w_0}{\partial \bar{x}^4} + (\bar{e}_0 \bar{a})^2 \left\{ -\frac{\partial}{\partial \bar{x}} \left(N_{\bar{x}} \frac{\partial w_0}{\partial \bar{x}} \right) + \frac{\partial}{\partial \bar{x}} \left(\bar{N}_0 \frac{\partial w_0}{\partial \bar{x}} \right) - Q + m_0 \frac{\partial^2 w_0}{\partial \bar{t}^2} - m_2 \frac{\partial^4 w_0}{\partial \bar{t}^2 \partial \bar{x}^2} \right\}$$

To obtain the equations of motion, Eq. (21) should be substituted into Eq. (13). Therefore, two following coupled equations are obtained

$$\begin{aligned}
&\delta u_0 : \frac{\partial}{\partial \bar{x}}\left(\left(\bar{A}_{\bar{x}\bar{x}}+\bar{A}_{\bar{x}\bar{x}\bar{t}}\frac{\partial}{\partial \bar{t}}\right)\left[\frac{\partial u_0}{\partial \bar{x}}-\bar{z}\frac{\partial^2 w_0}{\partial \bar{x}^2}+\frac{1}{2}\left(\frac{\partial w_0}{\partial \bar{x}}\right)^2\right]-\bar{R}_{68}+\right.\\
&\left.\frac{\partial}{\partial \bar{t}}\bar{R}_{79}-\left(\bar{A}_{\bar{x}\bar{x}}+\bar{A}_{\bar{x}\bar{x}\bar{t}}\frac{\partial}{\partial \bar{t}}\right)\bar{l}_m^2\left[\frac{\partial^3 u_0}{\partial \bar{x}^3}+\frac{\partial w_0}{\partial \bar{x}}\frac{\partial^3 w_0}{\partial \bar{x}^3}+\left(\frac{\partial^2 w_0}{\partial \bar{x}^2}\right)^2\right]\right)\\
&+\left(1-\left(\bar{e}_0\bar{a}\right)^2\nabla^2\right)F=\left(1-\left(\bar{e}_0\bar{a}\right)^2\nabla^2\right)m_0\frac{\partial^2 u_0}{\partial \bar{t}^2}
\end{aligned} \tag{22}$$

$$\begin{aligned}
&\delta w_0 : \left(\bar{D}_{\bar{x}\bar{x}}+\bar{D}_{\bar{x}\bar{x}\bar{t}}\frac{\partial}{\partial \bar{t}}\right)\left(1-\bar{l}_m^2\nabla^2\right)\frac{\partial^4 w_0}{\partial \bar{x}^4}+\left(1-\left(\bar{e}_0\bar{a}\right)^2\nabla^2\right)\times\\
&\left(\frac{\partial}{\partial \bar{x}}\left(N_{\bar{x}}\frac{\partial w_0}{\partial \bar{x}}\right)-\frac{\partial}{\partial \bar{x}}\left(\bar{N}_0\frac{\partial w_0}{\partial \bar{x}}\right)-Q\right)+\\
&\left(1-\left(\bar{e}_0\bar{a}\right)^2\nabla^2\right)\left(m_0\frac{\partial^2 w_0}{\partial \bar{t}^2}-m_2\frac{\partial^4 w_0}{\partial \bar{t}^2\partial \bar{x}^2}\right)=0
\end{aligned}$$

By neglecting the axial inertia and axial force from the first relation in Eq. (22) and implemented some simple manipulations, the force resultant $N_{\bar{x}}$ can be expressed as

$$\begin{aligned}
N_{\bar{x}\bar{x}}=&\left(\bar{A}_{\bar{x}\bar{x}}-\bar{A}_{\bar{x}\bar{x}\bar{t}}\frac{\partial}{\partial \bar{t}}\right)\left(\frac{1}{2L}\int_0^L\left(\frac{\partial w_0}{\partial \bar{x}}\right)^2 d\bar{x}-\right.\\
&\left.\frac{\bar{l}_m^2}{L}\int_0^L\left(\frac{\partial w_0}{\partial \bar{x}}\frac{\partial^3 w_0}{\partial \bar{x}^3}+\left(\frac{\partial w_0}{\partial \bar{x}}\right)^2\right)d\bar{x}-\bar{R}_{68}+\frac{\partial}{\partial \bar{t}}\bar{R}_{79}\right.
\end{aligned} \tag{23}$$

Thus replacing above equation for $N_{\bar{x}}$ in the second relation of Eq. (22), the equation of motion for a sandwich nano-beam with FG-CNTRC face-sheets based the nonlocal strain gradient theory yields as

$$\begin{aligned}
&\left(\bar{D}_{\bar{x}\bar{x}}+\bar{D}_{\bar{x}\bar{x}\bar{t}}\frac{\partial}{\partial \bar{t}}\right)\left(1-\bar{l}_m^2\nabla^2\right)\frac{\partial^4 w_0}{\partial \bar{x}^4}+\left(1-\left(\bar{e}_0\bar{a}\right)^2\nabla^2\right)\\
&\left(\bar{A}_{\bar{x}\bar{x}}+\bar{A}_{\bar{x}\bar{x}\bar{t}}\frac{\partial}{\partial \bar{t}}\right)\times\\
&\left(\frac{1}{2L}\int_0^L\left(\frac{\partial w_0}{\partial \bar{x}}\right)^2 d\bar{x}-\frac{\bar{l}_m^2}{L}\int_0^L\left(\frac{\partial w_0}{\partial \bar{x}}\frac{\partial^3 w_0}{\partial \bar{x}^3}+\left(\frac{\partial w_0}{\partial \bar{x}}\right)^2\right)d\bar{x}\right)\frac{\partial^2 w_0}{\partial \bar{x}^2}\\
&-\left(1-\left(\bar{e}_0\bar{a}\right)^2\nabla^2\right)\left(\bar{N}_0+\bar{R}_{68}+\frac{\partial}{\partial \bar{t}}\bar{R}_{79}\right)-\left(1-\left(\bar{e}_0\bar{a}\right)^2\nabla^2\right)\times\\
&Q\left(\bar{x},\bar{t}\right)+\left(1-\left(\bar{e}_0\bar{a}\right)^2\nabla^2\right)\left(m_0\frac{\partial^2 w_0}{\partial \bar{t}^2}-m_2\frac{\partial^4 w_0}{\partial \bar{t}^2\partial \bar{x}^2}\right)=0
\end{aligned} \tag{24}$$

3.2 External load

Effects of environment on the beam are simulated as Visco Pasternak foundation. Therefore the influence of the embedded environment is expressed as (Kanani *et al*. 2014)

$$f_e=-\bar{K}_w w_0+\bar{K}_s\frac{\partial^2 w_0}{\partial \bar{x}^2}-\bar{C}_d\frac{\partial w_0}{\partial \bar{t}}-\bar{K}_{nl}w_0^3 \tag{25}$$

In which, $\bar{K}_w$, $\bar{K}_s$, $\bar{K}_{nl}$ and $\bar{C}_d$ are Winkler stiffness coefficient, Pasternak shearing coefficient, nonlinear stiffness coefficient and viscos coefficient of the environment, respectively. In other hand, Maxwell's equation is expressed as

$$\begin{aligned}
&\bar{J}=\nabla\times\bar{h},\\
&\nabla\times\bar{e}=-\eta.\frac{\partial\bar{h}}{\partial t},\\
&div\,\bar{h}=0,\\
&\bar{e}=-\eta.\left(\frac{\partial\bar{U}}{\partial t}\times\bar{H}\right),\\
&\bar{h}=\nabla\times\left(\bar{U}\times\bar{H}\right),
\end{aligned} \tag{26}$$

In above equations, $\bar{h}$ is the disturbing vectors of magnetic field, $\bar{J}$ presents the current density, $\bar{e}$ represents the strength vectors of electric field and $\bar{U}$ characterizes the vector of displacement. In addition, ∇ demonstrates the Hamilton arithmetic operators where calculates as the form $\nabla=\frac{\partial}{\partial x}\bar{\imath}+\frac{\partial}{\partial x}\bar{\jmath}+\frac{\partial}{\partial x}\bar{k}$. The magnetic permeability is indicated by η. Herein, the longitudinal magnetic field vector applying on the carbon nanotube is specified as $\bar{H}=(H_{\bar{x}},0,0)$. If the displacement vector is defined as U = U (u, v, w) hence

$$\begin{aligned}
&\bar{h}=\nabla\times\left(\bar{U}\times\bar{H}\right)=-\bar{H}_x\left(\frac{\partial v}{\partial \bar{y}}+\frac{\partial w}{\partial \bar{z}}\right)\bar{\imath}+\bar{H}_x\frac{\partial v}{\partial \bar{y}}\bar{\jmath}+\bar{H}_x\frac{\partial w}{\partial \bar{y}}\bar{k}\\
&\bar{J}=\nabla\times\bar{h}=\bar{H}_{\bar{x}}\left(-\frac{\partial^2 v}{\partial \bar{x}\partial \bar{z}}+\frac{\partial^2 w}{\partial \bar{x}\partial \bar{y}}\right)\bar{\imath}-\bar{H}_x\left(\frac{\partial^2 v}{\partial \bar{y}\partial \bar{z}}+\frac{\partial^2 w}{\partial \bar{x}^2}+\frac{\partial^2 w}{\partial \bar{z}^2}\right)\bar{\jmath}+\\
&\bar{H}_x\left(\frac{\partial^2 v}{\partial \bar{x}^2}+\frac{\partial^2 v}{\partial \bar{y}^2}+\frac{\partial^2 w}{\partial \bar{y}\partial \bar{z}}\right)\bar{k}
\end{aligned} \tag{27}$$

Therefore, the components of the Lorentz force in $\bar{x}$, $\bar{y}$ and $\bar{z}$ directions are specified by the following form

$$\begin{aligned}
&f_{\bar{x}}=0\\
&f_{\bar{y}}=\eta\bar{H}_x^2\left(\frac{\partial^2 v}{\partial \bar{x}^2}+\frac{\partial^2 v}{\partial \bar{y}^2}+\frac{\partial^2 w}{\partial \bar{y}\partial \bar{z}}\right),\\
&f_{\bar{z}}=\eta\bar{H}_x^2\left(\frac{\partial^2 w}{\partial \bar{x}^2}+\frac{\partial^2 w}{\partial \bar{y}^2}+\frac{\partial^2 v}{\partial \bar{y}\partial \bar{z}}\right),
\end{aligned} \tag{28}$$

According to the defined displacement field in Eq. (3) and with attention to Eq. (28), only Lorentz force which applied on the carbon nano-tube embedded in sandwich nano-beam is specified as

$$f_z=\eta\bar{H}_x^2\left(\frac{\partial^2 w_0}{\partial \bar{x}^2}\right) \tag{29}$$

Substituting Eqs. (26), (27), (31) into Eq. (25) leads to governing equations of nonlinear vibration as

$$\begin{aligned}
&\left(\bar{D}_{\bar{x}\bar{x}}+\bar{D}_{\bar{x}\bar{x}\bar{t}}\frac{\partial}{\partial \bar{t}}\right)\left(1-\bar{l}_m^2\nabla^2\right)\frac{\partial^4 w_0}{\partial \bar{x}^4}-\left(1-\left(\bar{e}_0\bar{a}\right)^2\nabla^2\right)\\
&\left(\bar{A}_{\bar{x}\bar{x}}+\bar{A}_{\bar{x}\bar{x}\bar{t}}\frac{\partial}{\partial \bar{t}}\right)\times\\
&\left(\frac{1}{2L}\int_0^L\left(\frac{\partial w_0}{\partial \bar{x}}\right)^2 d\bar{x}-\frac{\bar{l}_m^2}{L}\int_0^L\left(\frac{\partial w_0}{\partial \bar{x}}\frac{\partial^3 w_0}{\partial \bar{x}^3}+\left(\frac{\partial w_0}{\partial \bar{x}}\right)^2\right)d\bar{x}\right)\frac{\partial^2 w_0}{\partial \bar{x}^2}\\
&+\left(1-\left(\bar{e}_0\bar{a}\right)^2\nabla^2\right)\left(\bar{N}_0+\bar{R}_{68}+\frac{\partial}{\partial \bar{t}}\bar{R}_{79}\right)+\left(1-\left(\bar{e}_0\bar{a}\right)^2\nabla^2\right)\times\\
&\left(\bar{K}_w w_0+\bar{K}_{nl}w_0^3-\bar{K}_s\frac{\partial^2 w_0}{\partial \bar{x}^2}+\bar{C}_d\frac{\partial w_0}{\partial \bar{t}}-\eta\bar{H}_x^2\left(\frac{\partial^2 w_0}{\partial \bar{x}^2}\right)\right)\\
&+\left(1-\left(\bar{e}_0\bar{a}\right)^2\nabla^2\right)\left(m_0\frac{\partial^2 w_0}{\partial \bar{t}^2}-m_2\frac{\partial^4 w_0}{\partial \bar{t}^2\partial \bar{x}^2}\right)=0
\end{aligned} \tag{30}$$

By defining following variables

$$x=\frac{\bar{x}}{L},\quad w=\frac{w_0}{h},\quad ,l_m=\frac{\bar{l}_m}{L},\quad ea=\frac{\bar{e}_0\bar{a}}{L},\quad t=\frac{\bar{t}}{T_0},\ T_0=\sqrt{\frac{m_0L^4}{\bar{D}_{\bar{x}\bar{x}}}},$$
$$K_w=\frac{\bar{K}_wL^4}{\bar{D}_{\bar{x}\bar{x}}},\quad K_s=\frac{\bar{K}_sL^2}{\bar{D}_{\bar{x}\bar{x}}},\quad K_{nl}=\frac{\bar{K}_{nl}L^4h^2}{\bar{D}_{\bar{x}\bar{x}}},\quad C_d=\frac{\bar{C}_dL^4}{T_0\bar{D}_{\bar{x}\bar{x}}},$$
$$A_{xx}=\frac{\bar{A}_{\bar{x}\bar{x}}L^2}{\bar{D}_{\bar{x}\bar{x}}}\left(\frac{h}{L}\right)^2,\quad D_{xx\tau}=\frac{\bar{D}_{\bar{x}\bar{x}\tau}}{\bar{D}_{\bar{x}\bar{x}}T_0},\quad R_{68}=\frac{\bar{R}_{68}L^2}{\bar{D}_{\bar{x}\bar{x}}},\quad R_{79}=\frac{\bar{R}_{79}L^2}{T_0\bar{D}_{\bar{x}\bar{x}}},$$
$$A_{xx}=\frac{\bar{A}_{\bar{x}\bar{x}}L^2}{T_0\bar{D}_{\bar{x}\bar{x}}}\left(\frac{h}{L}\right)^2 \tag{31}$$

The final dimensionless equation of motion is obtained as

$$x=\frac{\bar{x}}{L},\quad w=\frac{w_0}{h},\quad ,l_m=\frac{\bar{l}_m}{L},\quad ea=\frac{\bar{e}_0\bar{a}}{L},\quad t=\frac{\bar{t}}{T_0},\ T_0=\sqrt{\frac{m_0L^4}{\bar{D}_{\bar{x}\bar{x}}}},$$
$$K_w=\frac{\bar{K}_wL^4}{\bar{D}_{\bar{x}\bar{x}}},\quad K_s=\frac{\bar{K}_sL^2}{\bar{D}_{\bar{x}\bar{x}}},\quad K_{nl}=\frac{\bar{K}_{nl}L^4h^2}{\bar{D}_{\bar{x}\bar{x}}},\quad C_d=\frac{\bar{C}_dL^4}{T_0\bar{D}_{\bar{x}\bar{x}}},$$
$$A_{xx}=\frac{\bar{A}_{\bar{x}\bar{x}}L^2}{\bar{D}_{\bar{x}\bar{x}}}\left(\frac{h}{L}\right)^2,\quad D_{xx\tau}=\frac{\bar{D}_{\bar{x}\bar{x}\tau}}{\bar{D}_{\bar{x}\bar{x}}T_0},\quad R_{68}=\frac{\bar{R}_{68}L^2}{\bar{D}_{\bar{x}\bar{x}}},\quad R_{79}=\frac{\bar{R}_{79}L^2}{T_0\bar{D}_{\bar{x}\bar{x}}},$$
$$A_{xx}=\frac{\bar{A}_{\bar{x}\bar{x}}L^2}{T_0\bar{D}_{\bar{x}\bar{x}}}\left(\frac{h}{L}\right)^2 \tag{32}$$

4. Non-linear vibration analysis

4.1 Free vibration

In order to nonlinear free vibration analysis and studying the nonlinear vibration behaviors, Eq. (32) with considering mid plane stretching and pre-tension is rewritten as

$$\left(1+D_{xx\tau}\frac{\partial}{\partial t}\right)\left(1-l_m^2\nabla^2\right)\frac{\partial^4w}{\partial x^4}-\left(1-(ea)^2\nabla^2\right)\times$$
$$\left(A_{xx}+A_{xx\tau}\frac{\partial}{\partial t}\right)\times$$
$$\left(\frac{1}{2}\int_0^1\left(\frac{\partial w}{\partial x}\right)^2dx-l_m^2\int_0^1\left(\frac{\partial w}{\partial x}\frac{\partial^3w}{\partial x^3}+\left(\frac{\partial w}{\partial x}\right)^2\right)dx\right)\frac{\partial^2w}{\partial x^2}$$
$$+\left(1-(ea)^2\nabla^2\right)\left(N_0+R_{68}+\frac{\partial}{\partial t}R_{79}\right)+\left(1-(ea)^2\nabla^2\right)\times$$
$$\left(K_ww+K_{nl}w^3-\left(K_s+H_x\right)\frac{\partial^2w}{\partial x^2}+C_d\frac{\partial w}{\partial t}\right)$$
$$+\left(1-(ea)^2\nabla^2\right)\left(\frac{\partial^2w}{\partial t^2}-\bar{m}_2\frac{\partial^4w}{\partial t^2\partial x^2}\right)=0 \tag{33}$$

To solve equation of motion, decomposition Galerkin method is used to convert nonlinear partial differential equation (PDE) to nonlinear ordinary differential equation (ODE) (Ahmadian *et al.* 2009, Pirbodaghi *et al.* 2009, Asghari *et al.* 2010). For this aim, the solution of the Eq. (32) is assumed as

$$w(x,t)=w(x)q(t) \tag{34}$$

In Eq. (34), $q(t)$ is the time dependent amplitude for nonlinear vibration of the beam and $w(x)$ is assumed the linear fundamental vibration mode to satisfy boundary conditions. Then, substitution of Eq. (34) into Eq. (33) and using the decomposition Galerkin's method, the governing nonlinear ordinary differential equation of motion is obtained as

$$\ddot{q}(t)+A_1q(t)+A_2\dot{q}(t)+A_3q^3(t)+A_4\dot{q}(t)q^2(t)=0 \tag{35}$$

Where, coefficients presented in Eq. (40) are calculated by decomposition Galerkin method appeared in Appendix A2. The initial conditions for Eq. (40) are expressed as

$$q(0)=a_0,\quad \dot{q}(0)=0 \tag{36}$$

To solve Eq. (35), MTS method is employed with considering its initial condition represented in Eq. (36). According to aforementioned method, the response is assumed as 3rd order uniform expansion of multiple independent variables or time scales. Based on the following expressions, solution considered for Eq. (35) is assumed as (Nayfeh and Mook 2008)

$$q(\tau;\varepsilon)=\varepsilon q_0(T_0,T_1,T_2,)+\varepsilon^2q_1(T_0,T_1,T_2,)+$$
$$\varepsilon^3q_2(T_0,T_1,T_2,) \tag{37}$$

Where, ε is a measure of the amplitude of the motion (Hossieni *et al.* 2014). For this case, the independent time variables are introduced as

$$T_n=\varepsilon^n\tau\qquad n=0,1,2,....., \tag{38}$$

In which, $T_0=\tau$ is fast time scale and slow time scales are defined as $T_n=\epsilon^n\tau$, n ≥ 1. Fast time scale determines the main oscillatory behavior of the system (El-Borgi *et al.* 2015). By substituting Eq. (37) into Eq. (35), the system of linear equations based on the orders of ε is derived

$$\varepsilon^1: D_0^2q_1+A_1q_1=0$$
$$\varepsilon^2: D_0^2q_2+A_1q_2=-2D_0D_1q_1$$
$$\varepsilon^3: D_0^2q_3+A_1q_3=-(D_1^2+2D_2D_0)q_1-A_3{q_1}^3-$$
$$2D_0D_1q_2-A_4D_0q_1q_1^2-A_2D_0q_1 \tag{39}$$

Where, D_0, D_1 and D_2 defines derivatives $\frac{\partial}{\partial T_0}$, $\frac{\partial}{\partial T_1}$ and $\frac{\partial}{\partial T_2}$, and D_0^2, D_1^2 and D_2^2 represent $\frac{\partial^2}{\partial T_0^2}$, $\frac{\partial^2}{\partial T_1^2}$ and $\frac{\partial^2}{\partial T_2^2}$, respectively. Nayfeh and Mook analyzed ordinary differential equation with cubic and quadratic nonlinearities using the MTS method (Nayfeh and Mook 2008). After some simple manipulation, the closed form expression for the nonlinear frequency of the structure ignored the damping terms is calculated as follows

$$\omega_{nl}=\sqrt{A_1}\left(1+\frac{1}{8}\left(3\frac{A_3}{A_1}-\frac{A_4}{\sqrt{A_1}}\right)a_0^2\right) \tag{40}$$

And also the first approximation for time dependent amplitude of the nonlinear damping vibration yields as

$$q_0 = a_0 \exp\left(-\frac{1}{2}A_2 t\right)\cos\left(\sqrt{A_1}t - \left(\frac{3A_3 a_0^2}{8A_2\sqrt{A_1}} - \frac{1}{8}\frac{A_4}{A_2}a_0^2\right)\times \left(\exp(-A_2 t)-1\right)\right) \quad (41)$$

4.2 Forced vibration

In order to accomplish this analysis, the pretension force is assumed to vary with time as

$$N_0(t) = N_0\cos(\Omega t) \quad (42)$$

In which, Ω is the frequency of the pretention. Based on Eq. (40) the time dependent equation is expressed as

$$\ddot{q}(t) + A_{11}q(t) + A_{12}N_0(t)q(t) + A_2\dot{q}(t) + A_3 q^3(t) + A_4\dot{q}(t)q^2(t) = 0 \quad (43)$$

Where new coefficients $A_{11}$and A_{12} are represented in the Appendix A2. By substituting Eq. (37) into Eq. (42), the system of linear equations based on the orders of ε will is derived

$$\begin{aligned} &\varepsilon^1 : D_0^2 q_1 + A_{11}q_1 = 0 \\ &\varepsilon^2 : D_0^2 q_2 + A_{11}q_2 = -(A_{12}N_0(t) + 2D_1D_0)q_0 - A_2 D_0 q_0 - A_0 q_0^3 - A_4 D_0 q_0 q_0^2 \end{aligned} \quad (44)$$

According to solution procedure, primarily the first equation must be solve. Therefore, the solve of the aforementioned equation is achieved as

$$q_0 = B(T_1)\exp\left(\sqrt{A_{11}}T_0\right) + cc \quad (45)$$

Where, $B(T_1)$ is an unknown complex function of T_1 and cc denotes the complex conjugate of the preceding terms. Then Eq. (45) is replaced in the second relation of Eq. (44). The primary resonance is occurred when the frequency of excitation Ω is getting close to the linear frequency of the system ω_0 i.e., $\Omega \approx \omega_0$. This relation is described by the following equation

$$\Omega = \omega_0 + \varepsilon\sigma \quad (46)$$

Wherein σ is a detuning parameter and $\omega_0 = \sqrt{A_{11}}$. In order to eliminate secular terms from q_1 after substituting Eq. (45) into the second relation of Eq. (44), coefficient of $e^{i\omega T_0}$ must be equal to zero. Therefore following equation is obtained

$$-2\left(\frac{\partial B(T_1)}{\partial T_1}\right)i\sqrt{A_{11}} - A_2 i\sqrt{A_{11}}B(T_1) - A_3 B(T_1)^2\bar{B}(T_1) - A_4 i\sqrt{A_{11}}B(T_1)^2\bar{B}(T_1) - \frac{A_{12}}{2}N_0\bar{B}(T_1)\exp(i\sigma T_1) = 0 \quad (47)$$

Considering $B(T_1)$ in polar form as

$$B(T_1) = \frac{1}{2}a(T_1)e^{i\gamma(T_1)} \quad (48)$$

And substituting it into Eq. (47) yields

$$\begin{aligned} &-\frac{\partial a}{\partial T_1} - A_2\sqrt{A_{11}}a - \frac{1}{4}A_{12}N_0 a\cos\theta - \frac{1}{8}A_4\sqrt{A_{11}}a^3 = 0 \\ &\frac{\partial\gamma}{\partial T_1}\sqrt{A_{11}} - \frac{1}{8}A_3 a^2 - \frac{1}{4}A_{12}N_0\sin\theta = 0 \rightarrow \theta = \sigma T_2 - \gamma \end{aligned} \quad (49)$$

The point which $\frac{\partial a}{\partial T_1} = 0$ and $\frac{\partial\gamma}{\partial T_1} = 0$ corresponds to the singular point of the system and shows the steady-state motion of the system. After some manipulation, the steady state frequency response equation is expressed as

$$\left(4A_2\sqrt{A_{11}} + \frac{1}{2}A_4\sqrt{A_{11}}a^2\right)^2 + \left(a\sigma\sqrt{A_{11}} - \frac{1}{2}A_3 a^2\right) = (A_{12}N_0)^2 \quad (50)$$

5. Numerical results and discussion

5.1 Validation of the results

In this section, numerical results are presented for both nonlinear free and forced vibrations of the sandwich nano-beam with CNTRC face-sheets. The material properties and geometrical specifications of the beam are presented in Table 1. Herein, to justify the accuracy of the present issue, the results obtained in this research are compared with existing results of literature using ODE-45 method. Shown in Fig. 2 is the comparison between MTS method and numerical results obtained by ODE-45 method. According to these figures it is deduced that the current method has capability to evaluate the nonlinear time responses with acceptable accuracy. Another comparison is carried out to verify the reliability of the present formula and present solutions. For this aim, dimensionless natural frequency for a sandwich nano-beam with FG-CNTRC face-sheets is compared with results obtained from exact solution or reference (Gheshlaghi and Hasheminejad 2011). Table 2 presents the natural frequency of a sandwich nano-beam as a function of non-dimensional initial condition a_0 and also shows the comparison between the present results and analytical results.

It is necessary noted that based on the scientific principles of nonlinear vibrations, increasing the initial amplitude of initial conditions causes the nonlinear natural frequency of nonlinear vibration to increase. The semi analytical methods such as MTS method can't well take into account the effects of aforementioned phenomenon in the final solution for natural frequency. Therefore, regarding to results presented in Table 2, it can be concluded that increasing the initial amplitude causes the difference between the results obtained by the analytical method and the semi-analytical method to increase.

Table 1 The material and geometrical properties of the constituent material of the sandwich FG beam (Rafiee *et al*. 2013)

materials	Yang modules (Gp)	Expansion coefficient($1/C^o$)	Length(nm)	Height(nm)	d_{31}
piezoelectric	63	0.9e(-6)	20*H	100	2.54e(-10)
CNT	5.65e+3	3.4584e(-6)			-

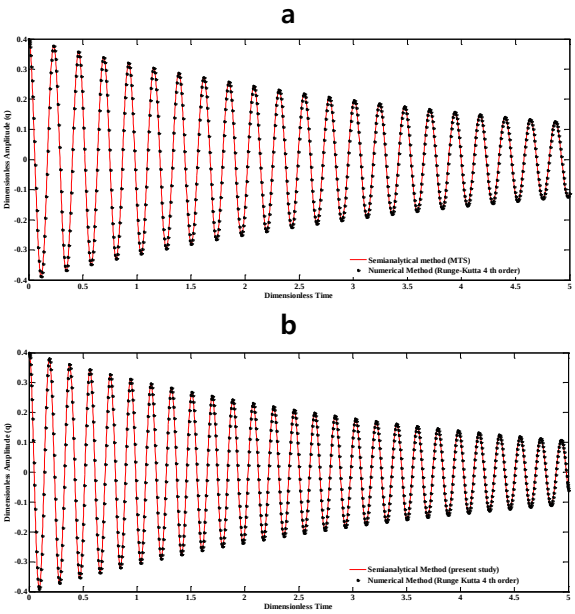

Fig. 2 Dimensionless Deflection of a. simply supported and b. clamped-clamped beam versus Dimensionless time (time-response)

5.2 Nonlinear free damping vibration

Considering Eq. (41) it can be concluded that unlike to the time response of the linear damping vibration, in the nonlinear damping vibration, the nonlinear damping frequency is a function of the initial condition (a_0) and the coefficient of damping (C_d). Table 3 shows that increasing the damping coefficient of Visco-elastic foundation leads to an important rise in the time periods. Furthermore, it leads to decrease of the nonlinear damping frequency of the vibration. Regard to the obtained results presented in Table. 4, the nonlinear damping frequency of the sandwich nano-beam associated to the first time period is increased by increasing the strain gradient parameter (l_m). In other hand, increase of the nonlocal parameter (ea) leads to decrease of the nonlinear damping frequency of the sandwich nano-beam.

The effects of the Winkler coefficient (K_w), the visco-elastic coefficient (τ_{cn}) and the applied voltage (V) on the nonlinear damping frequency are presented in table 5. According to these results, increase of the Winkler coefficient increases nonlinear damping frequency while nonlinear frequency is decreased by increase of Visco-elastic coefficient of the CNTs and the applied voltage.

Regard to results of Table 6, enhancing ΔT and N_0 have the same effect on nonlinear damping frequency. One can conclude that increase of the aforementioned parameters leads to decrease of nonlinear damping frequency. In addition, increase of shearing coefficient of the elastic foundation leads to increase of the nonlinear damping frequency.

The presented results in Table. 7 show influences of the various pattern of CNTs on nonlinear frequency. It can be concluded that AV pattern has a higher frequency with respect to other patterns and also according to these results the nonlinear damping frequency is enhanced by increase of the nonlinear stiffness of the elastic foundation and longitudinal magnetic field.

Table 2 The comparison between obtained results in present work and results of exact solution in Ref. (Gheshlaghi and Hasheminejad 2011)

Dimensionless Initial Amplitude (a_0)	Dimensionless nonlinear frequency (exact solution Ref. Gheshlaghi and Hasheminejad 2011)	Dimensionless nonlinear frequency (semi analytical solution (present work))	Error (%)
0.02	20.809	20.809	0.00
0.04	20.812	20.811	0.00
0.06	20.816	20.814	0.01
0.08	20.823	20.819	0.02
0.1	20.831	20.825	0.03
0.12	20.841	20.833	0.04
0.14	20.852	20.841	0.05
0.16	20.866	20.852	0.07
0.18	20.881	20.863	0.09
0.2	20.898	20.876	0.11

Table 3 The effect of the damping coefficient on nonlinear time periods

C_d	Time Period (1)	Time Period (2)	Time Period (3)
4.50	0.3016	0.3019	0.3019
6.75	0.3017	0.3019	0.302
8.99	0.3018	0.3019	0.302

Table 4 The effects of the nonlocal and strain gradient parameters on nonlinear damping frequency

Dimensionless Nonlinear Damping Frequency (ea= 0.06)					
Mode number	1	2	3	4	5
l_m= 0.01	22.89	28.35	62.85	111.06	166.64
l_m= 0.02	22.90	28.63	64.13	114.48	173.92
l_m= 0.03	22.91	29.10	66.19	119.97	185.42
l_m= 0.04	22.92	29.75	68.99	127.26	200.42
l_m= 0.05	22.94	30.56	72.41	136.06	218.20
Dimensionless Nonlinear Damping Frequency (ea = 0.08)					
Mode number	1	2	3	4	5
l_m= 0.01	22.84	26.11	54.59	93.23	136.27
l_m 0.02	22.84	26.39	55.82	96.41	142.78
l_m= 0.03	22.85	26.86	57.82	101.48	153.01
l_m= 0.04	22.87	27.49	60.50	108.19	166.28
l_m= 0.05	22.88	28.29	63.78	116.24	181.93
Dimensionless Nonlinear Damping Frequency (ea = 0.1)					
Mode number	1	2	3	4	5
l_m= 0.01	22.77	23.52	45.90	76.44	110.15
l_m= 0.02	22.78	23.80	47.11	79.46	116.11
l_m= 0.03	22.79	24.27	49.07	84.24	125.43
l_m= 0.04	22.80	24.90	51.69	90.51	137.42
l_m= 0.05	22.82	25.69	54.88	97.99	151.45

Table 5 The effects of K_w, τ_{cn} and V on nonlinear frequency

Dimensionless Nonlinear Damping Frequency (V = 0.5)					
τ_{cn}	0.0005	0.001	0.0016	0.0021	0.0026
K_w = 686.5	20.8690	20.8682	20.8673	20.8665	20.8656
K_w= 772.4	22.8362	22.8355	22.8349	22.8342	22.8335
K_w= 858.2	24.6468	24.6463	24.6457	24.6451	24.6446
K_w= 944.0	26.3332	26.3327	26.3322	26.3317	26.3313
K_w= 1029.8	27.9178	27.9174	27.9170	27.9166	27.9162
Dimensionless Nonlinear Damping Frequency (V = 0.3)					
τ_{cn}	0.0005	0.001	0.0016	0.0021	0.0026
K_w= 686.5	24.3184	24.3181	24.3177	24.3174	24.3171
K_w= 772.4	26.026	26.0258	26.0255	26.0252	26.025
K_w= 858.2	27.6282	27.628	27.6278	27.6276	27.6274
K_w= 944.0	29.1425	29.1423	29.1422	29.142	29.1418
K_w= 1029.8	30.5818	30.5817	30.5816	30.5814	30.5813
Dimensionless Nonlinear Damping Frequency (V = 0.1)					
τ_{cn}	0.0005	0.001	0.0016	0.0021	0.0026
K_w= 686.5	27.3356	27.3356	27.3357	27.3357	27.3357
K_w= 772.4	28.8652	28.8653	28.8653	28.8653	28.8654
K_w= 858.2	30.3177	30.3178	30.3178	30.3179	30.3179
K_w= 944.0	31.7037	31.7038	31.7039	31.7039	31.704
K_w= 1029.8	33.0316	33.0317	33.0318	33.0318	33.0319

Table 6 The effects of the K_s, N_0 and ΔT on nonlinear frequency

Dimensionless Nonlinear Damping Frequency ($T - T_0$ = 100)					
N_0	0.25	0.49	0.74	0.99	1.23
K_s= 0.9851	27.0221	26.977	26.9318	26.8866	26.8413
K_s= 1.9701	27.2017	27.1569	27.112	27.0671	27.0221
K_s= 2.9552	27.3801	27.3356	27.2911	27.2464	27.2017
K_s= 3.9402	27.5574	27.5132	27.4689	27.4246	27.3801
K_s= 4.9253	27.7335	27.6896	27.6456	27.6015	27.5574
Dimensionless Nonlinear Damping Frequency ($T - T_0$ = 200)					
N_0	0.25	0.49	0.74	0.99	1.23
K_s= 0.9851	26.9336	26.8884	26.8431	26.7977	26.7522
K_s= 1.9701	27.1138	27.0689	27.0239	26.9788	26.9336
K_s= 2.9552	27.2928	27.2482	27.2035	27.1587	27.1138
K_s= 3.9402	27.4706	27.4263	27.3819	27.3374	27.2928
K_s= 4.9253	27.6473	27.6033	27.5591	27.5149	27.4706
Dimensionless Nonlinear Damping Frequency ($T - T_0$ = 300)					
N_0	0.25	0.49	0.74	0.99	1.23
K_s= 0.9851	26.8449	26.7995	26.754	26.7085	26.6628
K_s= 1.9701	27.0256	26.9806	26.9354	26.8902	26.8449
K_s= 2.9552	27.2052	27.1604	27.1156	27.0706	27.0256
K_s= 3.9402	27.3836	27.3391	27.2946	27.2499	27.2052
K_s= 4.9253	27.5609	27.5167	27.4724	27.428	27.3836

Table 7 The effects of the K_{nl}, H_x and various pattern of CNTs on nonlinear frequency

Dimensionless Nonlinear Damping Frequency (VA pattern)					
K_{nl}	25	49	74	99	124
H_x = 0.1485	26.6212	26.6309	26.6405	26.6502	26.6598
H_x = 0.5939	26.7038	26.7134	26.723	26.7327	26.7423
H_x= 1.3362	26.8409	26.8505	26.86	26.8696	26.8792
H_x= 2.3755	27.0316	27.0411	27.0506	27.0602	27.0697
H_x= 3.7117	27.2749	27.2843	27.2937	27.3032	27.3126
Dimensionless Nonlinear Damping Frequency (UU pattern)					
K_{nl}	25	49	74	99	124
H_x= 0.1485	22.7464	22.7543	22.7621	22.7700	22.7779
H_x= 0.5939	22.8136	22.8214	22.8292	22.8371	22.8449
H_x= 1.3362	22.9250	22.9328	22.9406	22.9484	22.9562
H_x= 2.3755	23.0802	23.0879	23.0957	23.1034	23.1112
H_x= 3.7117	23.2781	23.2858	23.2935	23.3012	23.3089
Dimensionless Nonlinear Damping Frequency (AV pattern)					
K_{nl}	25	49	74	99	124
H_x= 0.1485	30.0563	30.0676	30.0790	30.0903	30.1016
H_x= 0.5939	30.1526	30.1638	30.1751	30.1864	30.1977
H_x= 1.3362	30.3122	30.3235	30.3347	30.3459	30.3572
H_x= 2.3755	30.5344	30.5456	30.5567	30.5679	30.5790
H_x= 3.7117	30.8177	30.8287	30.8398	30.8509	30.8619

Table 8 The effects of the non-linearity terms on damping frequency

Dimensionless Linear Damping Frequency										
N_0	**0.2463**	**0.4925**	**0.7388**	**0.9851**	**1.2313**	**1.4776**	**1.7239**	**1.9701**	**2.2164**	**2.4627**
K_w **=171.6**	7.4864	7.322	7.1539	6.9817	6.8051	6.6238	6.4374	6.2455	6.0475	5.8427
K_w**=343.3**	15.0981	15.0173	14.936	14.8543	14.7721	14.6895	14.6064	14.5228	14.4387	14.3542
K_w**=514.9**	19.9964	19.9355	19.8743	19.813	19.7515	19.6897	19.6278	19.5657	19.5034	19.4409
K_w**=686.5**	23.9116	23.8606	23.8095	23.7584	23.7071	23.6557	23.6042	23.5526	23.5008	23.449
K_w**=858.2**	27.2703	27.2256	27.1809	27.1361	27.0912	27.0462	27.0012	26.956	26.9108	26.8656
K_w**=1029.8**	30.2585	30.2182	30.1779	30.1375	30.0971	30.0567	30.0161	29.9756	29.9349	29.8942
K_w**=1201.5**	32.977	32.94	32.9031	32.866	32.829	32.7919	32.7547	32.7176	32.6803	32.6431
K_w**=1373.1**	35.4878	35.4535	35.4192	35.3848	35.3504	35.3159	35.2814	35.2469	35.2124	35.1778
K_w**=1544.7**	37.8324	37.8002	37.768	37.7358	37.7035	37.6712	37.6389	37.6065	37.5741	37.5417
K_w**=1716.4**	40.0399	40.0095	39.9791	39.9486	39.9181	39.8876	39.8571	39.8266	39.796	39.7654
Dimensionless Non-linear Damping Frequency										
N_0	**0.2463**	**0.4925**	**0.7388**	**0.9851**	**1.2313**	**1.4776**	**1.7239**	**1.9701**	**2.2164**	**2.4627**
K_w**=171.6**	7.6266	7.4645	7.2987	7.129	6.9551	6.7767	6.5933	6.4046	6.2101	6.0091
K_w**=343.3**	15.1786	15.0981	15.0172	14.9359	14.8541	14.7719	14.6892	14.606	14.5224	14.4382
K_w**=514.9**	20.0596	19.9988	19.9378	19.8766	19.8153	19.7537	19.692	19.63	19.5679	19.5056
K_w**=686.5**	23.9654	23.9145	23.8636	23.8125	23.7613	23.71	23.6586	23.6071	23.5555	23.5037
K_w**=858.2**	27.3181	27.2735	27.2288	27.184	27.1392	27.0943	27.0494	27.0043	26.9592	26.914
K_w**=1029.8**	30.3019	30.2617	30.2214	30.1811	30.1408	30.1004	30.0599	30.0194	29.9788	29.9382
K_w**=1201.5**	33.0171	32.9802	32.9433	32.9063	32.8693	32.8322	32.7951	32.758	32.7208	32.6836
K_w**=1373.1**	35.5253	35.491	35.4567	35.4224	35.388	35.3536	35.3191	35.2847	35.2501	35.2156
K_w**=1544.7**	37.8677	37.8356	37.8034	37.7712	37.7389	37.7067	37.6744	37.6421	37.6097	37.5773
K_w**=1716.4**	40.0735	40.0431	40.0127	39.9822	39.9518	39.9213	39.8908	39.8603	39.8297	39.7991

In order to represent the difference between linear and non-linear frequency, the obtained results in table 8 represent the natural damping frequency for two linear and non-linear states of a beam with the same material and geometry properties in two states. Regarding to the results, it can be concluded that the non-linear frequency of the FG sandwich beam is larger than linear frequency for all K_w and N_0 values.

In order to illustrate the effects of considering K_w and K_s coefficients as simultaneously, the non-linear damping frequency are calculated and presented in Fig. 3 with respect to K_w for various K_s coefficients. According to these results it can be concluded that considering K_w and K_s coefficients as have the significant effects on non-linear damping frequency. In the other hand, regarding to the presented results in Fig. 3 it can be seen, increasing K_w and K_s coefficients causes the non-linear damping frequency to increase.

5.3 The nonlinear forced vibration results

The influence of parameters of visco-elastic foundation on the frequency–response of sandwich nano-beam is presented in Fig. 4. It can be observed that the frequency–response curves bend to right due to nonlinear hardening phenomenon. According to this figure, it can be concluded that the degree of the bending right is basically consistent for different viscosity coefficients (C_d) and also influence of it on the hardening nonlinearity phenomenon is not remarkable. Furthermore, enhancing the viscoelastic damping coefficient leads to the resonance region makes narrow whilst it is approximately constant with variation of the other visco-elastic foundation parameters. Moreover, due to the nonlinearity of the analysis, the jump phenomenon coming from abrupt increase or decrease of the amplitude of the response by changing the foundation parameters is revealed in the figure.

Fig. 5 illustrates the effect of the pretension amplitude (N_0), applied voltage (V), various pattern of CNTs in face-sheets and magnetic field intensity (H_x) on the frequency response of simply-supported sandwich nano-beam. According to this figure, the hardening phenomena decreases with increasing the magnetic field intensity and therefore the jump phenomenon is more significant for the sandwich nano-beams with lower magnetic field intensity. This is due to increase of magnetic field intensity that reduces the stiffness of sandwich nano-beams. Furthermore, change of aforementioned parameter makes that the bifurcation point varies.

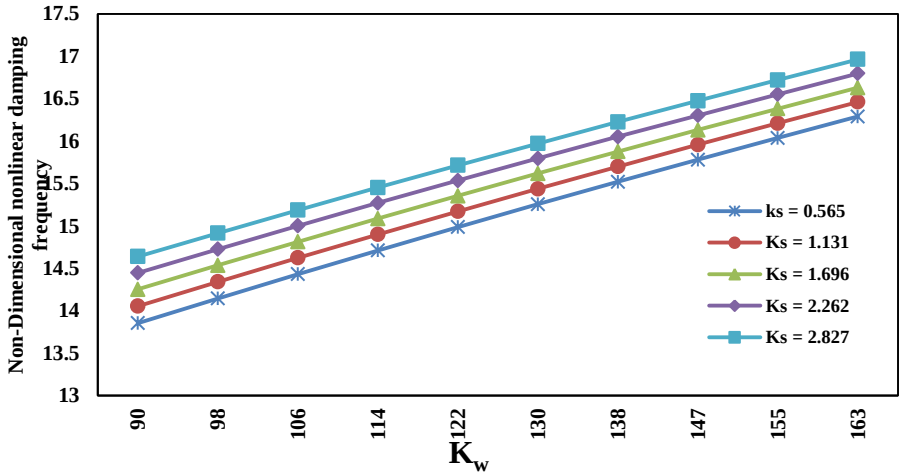

Fig. 3 the effects of the considering K_w and K_s coefficients simultaneously on non-linear damping frequency

Regard to Fig. 5, it can be concluded that increasing the pretension leads to increase of resonance region and consequently the point of nonlinear bifurcation phenomenon is changed. The influence of applied voltage on nonlinear frequency response is increase of the nonlinear hardening phenomenon as possibility of the jump phenomenon enhances. According to results of Fig. 5, the AV pattern has a frequency response with more obvious hardening phenomenon respect to other pattern.

The influences of the nonlocal and strain gradient parameters on nonlinear frequency response are investigated in Fig. 6. It is concluded that aforementioned parameters have no effect on location of the point occurred nonlinear bifurcation phenomenon.

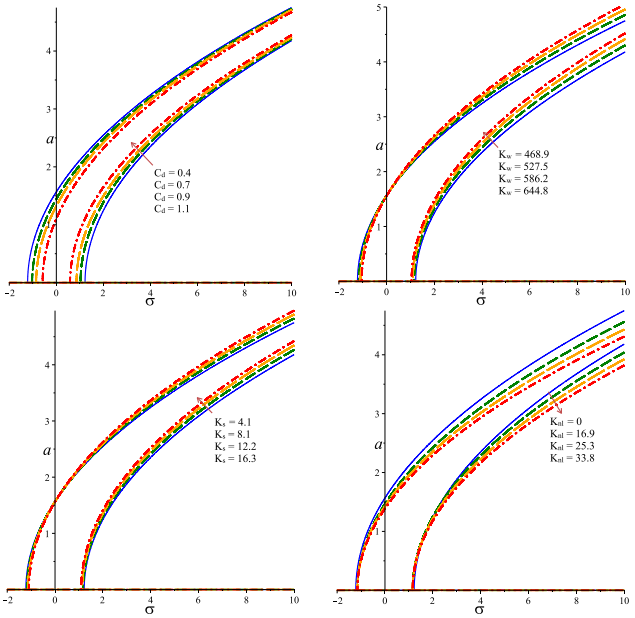

Fig. 4 The effect of parameters related to visco-elastic foundation on the frequency response

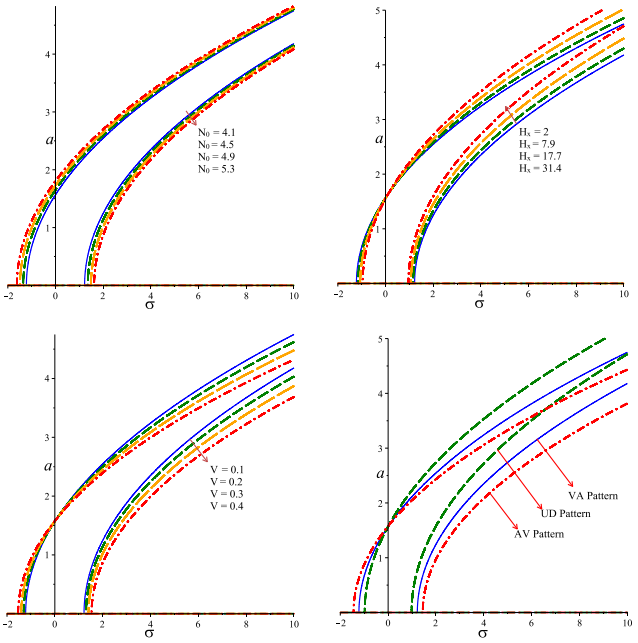

Fig. 5 The effect of the pretension, applied voltage, various pattern of CNTs in face-sheets and magnetic field intensity on the frequency response

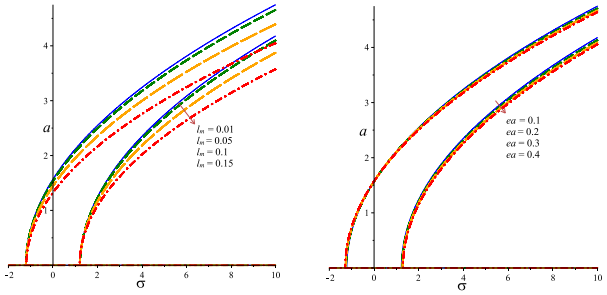

Fig. 6 The effect of the nonlocal (ea) and strain gradient (l_m) parameters on the frequency response

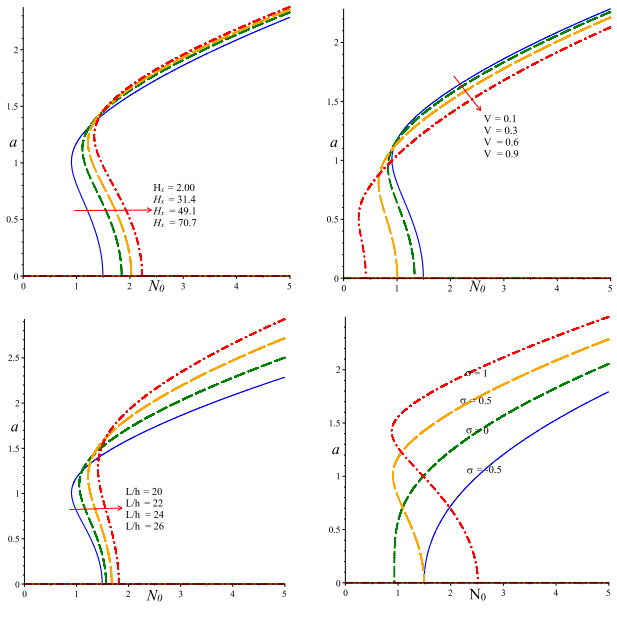

Fig. 7 The effect of the magnetic field intensity, applied voltage, slenderness ratio and detuning parameter on the force response

In addition, increasing these parameters causes that the nonlinear hardening phenomenon becomes more obvious of course according to figure the effects of the strain gradient parameter is more than the nonlocal parameter.

The nonlinear force response of the sandwich nano-beam with FG-CNTRC face-sheet is represented in Fig. 7. According to this figure it is concluded that the point of jump phenomenon is varied by changing the magnetic field intensity (H_x), applied voltage (V), slenderness ratio (L/h) and detuning parameter (σ). Regard to this figure, the force response can be converted to a safe force response (removing the nonlinear jump phenomenon from force response) by changing aforementioned parameters. For example according to this figure, increase of the slender ratio causes the force response converted to a safe force response diagram.

6. Conclusions

Analysis of the nonlinear free damping and parametric forced vibration of sandwich nano-beams with FG-CNTs face-sheets was implemented in this paper. The Euler–Bernoulli beam theory and Von-Karman nonlinear relations were used for this analysis. The mid-plan stretching and pretension was considered in equations of motion and also the nonlocal strain gradient theory to involve the nonlocal and strain gradient parameters. The equations of motion were solved by the semi analytical method (Multiple Times Scale) and the time, frequency and force response for nonlinear free and forced vibration were derived. The effects of some parameters such as length scale parameters, different distribution pattern of CNTs in face-sheets, parameters of Visco-Pasternak foundation, visco-elastic coefficients of the piezoelectric matrix and CNTs, different patterns of CNTs along the face-sheets, applied voltage, longitudinal magnetic field and other important parameters in designing and controlling the nonlinear damping vibration and phase velocity were studied in detail. The most important results of this study are presented as:

1. Volume fraction of the CNTs in face-sheets can strongly change nonlinear damping frequency of the sandwich nano-beam. The numerical results indicate that distribution patterns of CNTs have significant influence on the nonlinear damping frequency as the FG-AV possesses a more frequency value respect to other patterns. Aforementioned result was justified in the nonlinear frequency response results as regarding to the results the FG-AV pattern have a lower the response amplitude in comparison with other CNTs patterns.
2. The small scale parameters have significant effects on the nonlinear damping frequency of the nano-beam with FG-CNTRC face sheets. It can be observed that, increasing the nonlocal parameter will reduce the nonlinear damping frequency. Unlike to nonlocal parameter, increment of the strain gradient parameter leads to enhance in the nonlinear damping frequency. This results was validated in the nonlinear frequency response of the nano-beam, correctly.
3. Investigation on the effect of parameters of Visco-Pasternak foundation on the nonlinear frequency response of the sandwich nano-beam leads to important conclusions. The hardening phenomenon became clearer with raising the nonlinear stiffness coefficient (K_{nl}) of the visco-Pasternak foundation and hardening property reduces by increase of the Winkler (K_w) and shearing (K_s) coefficients. In addition aforementioned parameters approximately have no effect on the point occurred the nonlinear bifurcation. According to obtained results, it concluded that the degree of the bending right is basically consistent for different viscosity coefficients of the visco-elastic foundation.

According to obtained results, the applied voltage, longitudinal magnetic field and increment temperature have important influences on nonlinear damping frequency and phase velocity. Increasing the increment temperature and applied voltage leads to decreasing phase velocity and nonlinear damping frequency, also they will enhance with increasing longitudinal magnetic field.

Acknowledgments

The author would like to thank the reviewers for their comments and suggestions to improve the clarity of this article. This work was supported by University of Kashan [Grant Number 574600/42].

References

Ahmadian, M.T., Mojahedi, M. and Moeenfard, H. (2009), “Free vibration analysis of a nonlinear beam using homotopy and modified lindstedt-poincare methods”, *J. Solid. Mech.*, **1**, 29-36.

Akgoz, B. and Civalek, O. (2013), “Longitudinal vibration

analysis of strain gradient bars made of functionally graded materials (fgm) ", *Compos. Part B: Eng.*, **55**, 263-268.
Akgoz, B. and Civalek, O. (2014), "Thermo-mechanical buckling behavior of functionally graded microbeams embedded in elastic medium", *Int. J. Eng. Sci*., **85**, 90-104.
Alibeigloo, A. (2014), "Three-dimensional thermoelasticity solution of functionally graded carbon nanotube reinforced composite plate embedded in piezoelectric sensor and actuator layers", *Compos. Struct.*, **118**, 482-495.
Amal, M.K.E. and Mahmoud, M.F. (2007), "Carbon nanotube reinforced composites: Potential and current challenges", *Mater. Des*., **28,** 2394-2401.
Ansari, R., Faghih Shojaei, M., Mohammadi, V., Gholami, R. and Sadeghi, S. (2014), "Nonlinear forced vibration analysis of functionally graded carbon nanotube-reinforced composite Timoshenko beams", *Compos. Struct*., **113,** 316-327.
Ansari, R., Shojaei, M.F., Mohammadi, V., Gholami, R. and Darabi, M.A. (2014), "Nonlinear vibrations of functionally graded mindlin microplates based on the modified couple stress theory", *Compos. Struct*., **114**, 124-134.
Arefi, M. (2016), "Surface effect and non-local elasticity in wave propagation of functionally graded piezoelectric nano-rod excited to applied voltage", *Appl. Math. Mech.*, **37**, 289-302.
Arefi, M., Pourjamshidian, M. and Ghorbanpour Arani, A. (2018), "Nonlinear free and forced vibration analysis of embedded functionally graded sandwich micro beam with moving mass", *J. Sandw. Struct. Mater.*, **20** (4), 462-492.
Arefi, M. and Zenkour, A.M. (2016), "Free vibration, wave propagation and tension analyses of a sandwich micro/nano rod subjected to electric potential using strain gradient theory", *Mater.Res.Express*., **3**(11), 115704.
Arefi, M. and Zenkour, A.M. (2017a), "Thermo-electro-mechanical bending behavior of sandwich nanoplate integrated with piezoelectric face-sheets based on trigonometric plate theory", *Compos. Struct.*, **162**, 108-122.
Arefi, M. and Zenkour, A.M. (2017b), "Effect of thermo-magneto-electro-mechanical fields on the bending behaviors of a three-layered nanoplate based on sinusoidal shear-deformation plate theory", *J. Sandw. Struct. Mater*., Doi: 1099636217697497.
Arefi, M. and Zenkour, A.M. (2017c), "Employing the coupled stress components and surface elasticity for nonlocal solution of wave propagation of a functionally graded piezoelectric Love nanorod model", *J. Intel. Mat. Syst. Str*., **28**(17), 2403-2413.
Arefi, M. and Zenkour, A.M. (2017d), "Size-dependent vibration and bending analyses of the piezomagnetic three-layer nanobeams", *Appl. Phys. A*., **123**(3), 202.
Arefi, M. and Zenkour, A.M. (2017e), "Vibration and bending analysis of a sandwich microbeam with two integrated piezo-magnetic face-sheets", *Compos. Struct*., **159**, 479-490.
Asghari, M., et al. (2010), "A nonlinear Timoshenko beam formulation based on the modified couple stress theory", *Int. J. Eng Sci*., **48,** 1749-1761.
Ashrafi, B. and Hubert, P. (2006), "Vengallatore S. Carbon nanotube-reinforced composites as structural materials for microactuators in microelectromechanical systems", *Nanotechnology*, **17**, 4895-4903.
Ebrahimi, F. and Salari, E. (2015), "Size-dependent free flexural vibrational behavior of functionally graded nanobeams using semi-analytical differential transform method", *Compos Part B: Eng.*, **79**, 156-169.
El-Borgi, S., Fernandes, R. and Reddy J.N. (2015). "Nonlocal Free and Forced Vibrations of Graded Nanobeams Resting on a Nonlinear Elastic Foundation", *Int. J. Nonlinear. Mech.* **77**, 348-363.
Esawi, A. and Farag, M. (2007), "Carbon nanotube reinforced composites: potential and current challenges", *Mater. Design***,** **28**, 2394-2401.
Fidelusa, J.D., Wiesela, E., Gojnyb, F.H., Schulteb, K. and Wagner, H.D. (2005), "Thermo-mechanical properties of randomly oriented carbon/epoxy nanocomposites", *Compos. Part A-Appl*., **36**, 1555-1561.
Formica, G., Lacarbonara, W. and Alessi, R. (2010), "Vibrations of carbon nanotube-reinforced composites", *J. Sound. Vib*., **329**, 1875-1889.
Gheshlaghi, B. and Hasheminejad, S.M. (2011), "Surface effects on nonlinear free vibration of nanobeams", *Compos. Part. B.*, **42**, 934-937.
Gholami, R., Darvizeh, A., Ansari, R. and Hosseinzadeh, M. (2014), "Sizedependent axial buckling analysis of functionally graded circular cylindrical microshells based on the modified strain gradient elasticity theory", *Meccanica*. **49**(7), 1679-1695.
Ghorbanpour Arani, A., Kolahchi, R. and Esmailpour, M. (2016), "Nonlinear vibration analysis of piezoelectric plates reinforced with carbon nanotubes using DQM", *Smart. Struct. Syst*., **18**(4), 787-800.
Ghorbanpour Arani, A., Vossough, H. and Kolahchi, R. (2015), "Nonlinear vibration and instability of a visco-Pasternak coupled double-DWBNNTs-reinforced microplate system conveying microflow", *J. Mech. Eng.* Sci., 1-17.
Ghorbanpour Arani, A., Vossough, H., Kolahchi, R. and Mosallaie Barzoki, A.A. (2012), "Electro-thermo nonlocal nonlinear vibration in an embedded polymeric piezoelectric micro plate reinforced by DWBNNTs using DQM", *J. Mech. Sci. Tech*., **26** (10), 3047-3057.
Hosseini, S.M., Mareishi, S., Kalhori, H. and Rafiee, M. (2014). "Large Amplitude Free and Forced Oscillations of Functionally Graded Beams", *Mech. Adv. Mater. Struct.*, **21**, 255–262.
Jam, J.E. and Kiani, Y. (2015), "Low velocity impact response of functionally graded carbon nanotube reinforced composite beams in thermal environment", *Compos. Struct.*, **132,** 35-43.
Jung, W.Y. and Han, S.C. (2015), "Static and eigenvalue problems of sigmoid functionally graded materials (s-fgm) micro-scale plates using the modified couple stress theory", *Appl. Math. Model*., **39**(12), 3506-3524.
Kanani, A.S., Niknam, H., Ohadi, A.R. and Aghdam, M.M. (2014), "Effect of nonlinear elastic foundation on large amplitude free and forced vibration of functionally graded beam", *Compos. Struct.*, **115**, 60-68.
Ke, L.L., Yang, J. and Kitipornchai, S. (2010), "Nonlinear free vibration of functionally graded carbon nanotube-reinforced composite beams", *Compos. Struct.*, **92,** 676-683.
Kiani, K. (2015), "Wave characteristics in aligned forests of single-walled carbon nanotubes using nonlocal discrete and continuous theories", *Int. J. Mech. Sci.*, **90**, 278-309.
Li, L. and Hu, Y. (2016), "Wave propagation in fluid-conveying viscoelastic carbon nanotubes based on nonlocal strain gradient theory", *Comp. Mater. Sci*., **112,** 282-288.
Li, L, Hu, Y. and Ling, L. (2015), "Flexural wave propagation in small-scaled functionally graded beams via a nonlocal strain gradient theory", *Compos. Struct.*, **133**, 1079-1092.
Li, L., Hu, Y. and Ling, L. (2015), "Wave propagation in viscoelastic single-walled carbon nanotubes with surface effect under magnetic field based on nonlocal strain gradient theory", *Physica E*, **75**, 118-124.
Li, Y., Wang, S., Wang, Q. and Xing, M. (2016), "Molecular dynamics simulations of tribology properties of NBR (Nitrile-Butadiene Rubber) /carbon nanotube composites", *Compos. Part B: Eng*., **97**, 62-67.
Liew, K.M., Hu, Y.G. and He, X.Q. (2008), "Flexural wave propagation in single-walled carbon nanotubes", *J. Comput. Theor. Nanosci*., **5**(4), 581-586.
Liew, K.M., Yang, J. and Kitipornchai, S. (2003), "Postbuckling of piezoelectric FGM plates subject to thermo-electro-mechanical loading", *Int. J. Solids. Struct*., **40**, 3869-3892.

Mohammadimehr, M. and Mostafavifar, M. (2016), "Free vibration analysis of sandwich plate with a transversely flexible core and FG-CNTs reinforced nanocomposite face sheets subjected to magnetic field and temperature-dependent material properties using SGT", *Compos. Part B: Eng*., **94**, 253-270.

Mohammadimehr, M., Rousta Navi, B. and Ghorbanpour Arani, A. (2015), "Free vibration of viscoelastic double-bonded polymeric nanocomposite plates reinforced by FG-SWCNTs using MSGT, sinusoidal shear deformation theory and meshless method", *Compos. Struct*., **131**, 654-671.

Mohammadimehr, M., Rousta Navi, B. and Ghorbanpour Arani, A. (2016), "Modified strain gradient Reddy rectangular plate model for biaxial buckling and bending analysis of double-coupled piezoelectric polymeric nanocomposite reinforced by FG-SWNT", *Compos. Part B: Eng*., **87**, 132-148

Natarajan, S., Haboussi, M. and Manickam, G. (2014), "Application of higher-order structural theory to bending and free vibration analysis of sandwich plates with CNT reinforced composite", *Compos. Struct*., **113,** 197-207.

Nateghi, A. and Salamat-talab, M. (2013), "Thermal effect on size dependent behavior of functionally graded microbeams based on modified couple stress theory", *Compos. Struct*., **96**, 97-110.

Nayfeh, A.H. and Mook, D.T. (2008), *Nonlinear Oscillations*, Wiley-VCH.

Nazemnezhad, R., Hosseini and Hashemi, S. (2014), "Nonlocal nonlinear free vibration of functionally graded nanobeams", *Compos. Struct*., **110**, 192-199.

Niknam, H. and Aghdam, M.M. (2015), "A semi analytical approach for large amplitude free vibration and buckling of nonlocal FG beams resting on elastic foundation", *Compos. Struct.*, **119**, 452-462.

Pang, M., Zhang, Y.Q. and Chen, W.Q. (2015), "Transverse wave propagation in viscoelastic single-walled carbon nanotubes with small scale and surface effects", *J. Appl. Phys*., **117**, 024305.

Pirbodaghi, T., Ahmadian, M.T. and Fesanghary, M. (2009), "On the homotopy analysis method for non-linear vibration of beams", *Mech. Res. Commun.*, **36**, 143-148.

Rafiee, M., He, X.Q. and Liew, K.M. (2014), "Non-linear dynamic stability of piezoelectric functionally graded carbon nanotube-reinforced composite plates with initial geometric imperfection", *Int. J. Nonlinear. Mech*., **59,** 37-51.

Rafiee, M., Yang, J. and Kitipornchai, S. (2013), "Large amplitude vibration of carbon nanotube reinforced functionally graded composite beams with piezoelectric layers", *Compos. Struct*., **96,** 716-725.

Rahmani, O. and Jandaghian, A.A. (2015), "Buckling analysis of functionally graded nanobeams based on a nonlocal third-order shear deformation theory", *Appl. Phys. A*., **119**(3), 1019-1032.

Reddy, J.N., El-Borgi, S. and Romanoff, J. (2014), "Non-linear analysis of functionally graded microbeams using eringens non-local differential model", *Int. J. Nonlinear. Mech*., **67**, 308-318.

Salehipour, H., Shahidi, A.R. and Nahvi, H. (2015). "Modified nonlocal elasticity theory for functionally graded materials", *Int. J. Eng. Sci*., **90**, 44-57.

Setoodeh, A. and Afrahim, S. (2014), "Nonlinear dynamic analysis of fg micro-pipes conveying fluid based on strain gradient theory", *Compos. Struct*., **116**, 128-135.

Shakeri, M., Akhlaghi, M. and Hoseini, S.M. (2006), "Vibration and radial wave propagation velocity in functionally graded thick hollow cylinder", *Compos. Struct*., **76**(1), 174-181.

Shen, H.S. and Zhang, C.L. (2010). "Thermal buckling and postbuckling behavior of functionally graded carbon nanotube-reinforced composite plates", *Mater. Design***, 31,** 3403-3411.

Shen, H.S. and Zhang, C.L. (2012), "Non-linear analysis of functionally graded fiber reinforced composite laminated plates, Part I: Theory and solutions", *Int. J. Nonlinear. Mech*., **47,** 1045-1054.

Simsek, M. and Yurtcu, H.H. (2013), "Analytical solutions for bending and buckling of functionally graded nanobeams based on the nonlocal timoshenko beam theory", *Compos. Struct*., **97**, 378-386.

Tajalli, S.A., Rahaeifard, M., Kahrobaiyan, M.H., Movahhedy, M.R., Akbari, J. and Ahmadian, M.T. (2013), "Mechanical behavior analysis of size-dependent micro-scaled functionally graded timoshenko beams by strain gradient elasticity theory", *Compos. Struct*., **102**, 72-80.

Wattanasakulpong, N. and Ungbhakorn, V. (2013), "Analytical solutions for bending, buckling and vibration responses of carbon nanotube-reinforced composite beams resting on elastic foundation", *Comp. Mater. Sci*., **71,** 201-208.

Wu, H., Yang, J. and Kitipornchai, S. (2016), "Nonlinear vibration of functionally graded carbon nanotube-reinforced composite beams with geometric imperfections SGT", *Compos. Part B: Eng*., **90**, 86-96.

Zenkour, A.M. and Arefi, M. (2017), "Nonlocal transient electrothermomechanical vibration and bending analysis of a functionally graded piezoelectric single-layered nanosheet rest on visco-Pasternak foundation", *J. Therm. Stresses*., **40**, 167-184.

Zhang, Z.J. and Paulino, G.H. (2007), "Wave propagation and dynamic analysis of smoothly graded heterogeneous continua using graded finite elements", *Int. J. Solids. Struct.***, 44**(11), 3601–3626.

CC

Appendix A

A1:

$$\begin{Bmatrix}\sigma_x\\ \sigma_x\\ \tau_{xz}\\ \tau_{zx}\\ \tau_{xy}\end{Bmatrix}=\begin{pmatrix}0 & 0 & e_{31}\\ 0 & 0 & e_{32}\\ 0 & 0 & 0\\ 0 & e_{24} & 0\\ e_{15} & 0 & 0\end{pmatrix}\begin{Bmatrix}E_x\\ E_y\\ E_z\end{Bmatrix} \tag{1}$$

$$e_{31}=Ed_{31} \tag{2}$$

$$E_i=-\frac{\partial\phi}{\partial i},i=x,y,z \tag{3}$$

$$\phi(x,z)=\frac{V(t)}{h}z \tag{4}$$

$$E_z=-\frac{\partial\phi}{\partial z}=-\frac{V(t)}{h} \tag{5}$$

A2:

$$A_2=\frac{\int_0^1\begin{pmatrix}C_d\left(w(x)-(ea_0)^2w''(x)\right)-\\ (R_{79})\left(w''(x)-(ea_0)^2w^{(4)}(x)\right)-\\ \left(D_{xx\tau}\right)\left(w^{(4)}(x)-l^2w^{(6)}(x)\right)\end{pmatrix}w(x)dx}{\int_0^1\begin{pmatrix}\left(w(x)-(ea)^2w''(x)\right)-\\ \bar{m}_2\left(w''(x)-(ea)^2w^{(4)}(x)\right)\end{pmatrix}w(x)dx} \tag{1}$$

$$A_1=\frac{\int_0^1\begin{pmatrix}K_w\left(w(x)-(ea)^2w''(x)\right)+\\ (R_{68})\left(w''(x)-(ea)^2w^{(4)}(x)\right)+\\ \left(w^{(4)}(x)-l_m{}^2w^{(6)}(x)\right)-\\ K_s\left(w''(x)-(ea)^2w^{(4)}(x)\right)-\\ N_0\left(w''(x)-(ea)^2w^{(4)}(x)\right)-\\ H_x\left(w''(x)-(ea_0)^2w^{(4)}(x)\right)\end{pmatrix}w(x)dx}{\int_0^1\begin{pmatrix}\left(w(x)-(ea)^2w''(x)\right)-\\ \bar{m}_2\left(w''(x)-(ea)^2w^{(4)}(x)\right)\end{pmatrix}w(x)dx}$$

$$A_3=\frac{\int_0^1w'(x)^2dx\int_0^1\left(w''(x)-(ea)^2w^{(4)}(x)\right)w(x)dx}{\int_0^1\begin{pmatrix}\left(w(x)-(ea)^2w''(x)\right)-\\ \bar{m}_2\left(w''(x)-(ea)^2w^{(4)}(x)\right)\end{pmatrix}w(x)dx}$$

$$A_4=\frac{\int_0^1w'(x)^2dx\int_0^1\left(w''(x)-(ea)^2w^{(4)}(x)\right)w(x)dx}{\int_0^1\begin{pmatrix}\left(w(x)-(ea)^2w''(x)\right)-\\ \bar{m}_2\left(w''(x)-(ea)^2w^{(4)}(x)\right)\end{pmatrix}w(x)dx}$$

Abbreviation

Table 8 Abbreviation

FG	functionally graded
CNTs	carbon nanotubes
PDE	partial differential equation
ODE	ordinary differential equation
MTS	Multiple Times Scale
UD	uniform distribution
SWCNT	single-walled carbon nanotube
CFs	carbon fibers
CNTRCs	carbon nanotube-reinforced composites
MEMS	micro-electro-mechanical systems
NEMS	nano-electro-mechanical systems
MLPG	meshless local Petrov–Galerkin